analytical chemistry

Article

pubs.acs.org/ac

Affinity Comparison of p3 and p8 Peptide Displaying Bacteriophages Using Surface Plasmon Resonance

Karel Knez,[†] Wim Noppe,[‡] Nick Geukens,[§] Kris P. F. Janssen,[†] Dragana Spasic,[†] Jeroen Heyligen,[†] Kim Vriens,[∥] Karin Thevissen,[∥] Bruno P. A. Cammue,[∥] Valery Petrenko,[⊥] Chris Ulens,[⊗] Hans Deckmyn,[‡,§] and Jeroen Lammertyn*[,†]

[†]BIOSYST-MeBioS, KU Leuven, Willem De Croylaan 42, P.O. Box 2428, B-3001 Leuven, Belgium

[‡]IRF Life Siences, KU Leuven Kulak, E. Sabbelaan 53, B-8500 Kortrijk, Belgium

[§]PharmAbs, The KU Leuven Antibody Center, O&N II, Herestraat 49, P.O. Box 824, B-3000 Leuven, Belgium

[∥]Centre for Microbial and Plant Genetics, KU Leuven, Kasteelpark Arenberg 20, P.O. 2460, B-3001 Heverlee, Belgium

[⊥]Auburn University, College of Veterinary Medicine, Department of Pathobiology, 269 Greene Hall, Auburn, Alabama 36849-5519, United States

[⊗]Laboratory for Structural Neurobiology, KU Leuven, O&N I, Herestraat 49, P.O. Box 601, B-3000 Leuven, Belgium

Supporting Information

ABSTRACT: Ever increasing demands in sensitivity and specificity of biosensors have recently established a trend toward the use of multivalent bioreceptors. This trend has also been introduced in the field of bacteriophage affinity peptides, where the entire phage is used as a receptor rather than the individual peptides. Although this approach is gaining in popularity due to the numerous advantages, binding kinetics of complete phage particles have never been studied in detail, notwithstanding being essential for the efficient design of such applications. In this paper we used an in house developed fiber-optic surface plasmon resonance (FO-SPR) biosensor to study the affinity and binding kinetics of phages, displaying peptide libraries. By using either peptide expression on the p3 or on the p8 coat proteins, a corresponding density of 5 up to more than 2000 peptides on a single virus particle was obtained. Binding parameters of 26 different filamentous phages, displaying peptides selective for enhanced Green Fluorescent Protein (eGFP), were characterized. This study revealed a broad affinity range of phages for the target eGFP, indicating their potential to be used for applications with different requirements in binding kinetics. Moreover, detailed analysis of k_{off} and k_{on} values of several selected p3 and p8 phages, using the FO-SPR biosensor, clearly showed the correlation between the binding parameters and the density at which eGFP-peptides are being expressed. Consequently, although p3 and p8-based phages both revealed exceptionally high affinities for eGFP, two p8 phages were found to have the highest affinity with dissociation constants (K_d) in the femtomolar range.

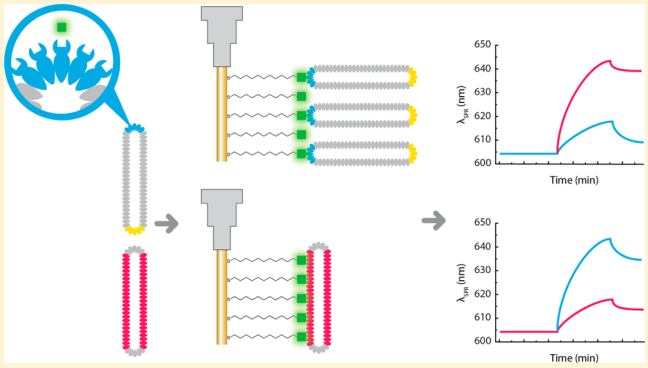

The interest in multivalent bioreceptors has been increasing in the last years with applications acknowledged in very diverse research fields, such as cell biology, where their role was studied in the process of cell attachment,[1] cell receptor clustering,[2] and molecular motion[3] but as well in the fields of drug development,[4] affinity chromatography,[5] and biosensors.[6] The concept of using multivalent bioreceptors due to their higher selectivity toward a target of interest[7] became especially appealing in the biosensors field, as the ever-increasing demands on the performance of biosensors continuously drives research toward more selective and sensitive receptors. Recently, it was even shown that immobilizing receptors, namely, antibodies, at high densities of more than 100 000 receptor copies per magnetic particle, allows one to control binding kinetics, resulting in extremely low dissociation constants (K_d) in the femtomolar range.[8]

This trend has recently been introduced in the field of filamentous phage particles, which can express multiple receptors on their surface through one of their five unique coat proteins, promoting thereby usage of the entire phage as a receptor rather than the individual proteins.[9] The most used coat proteins, as illustrated in Figure 1, are the minor coat protein p3, present in 5 copies at the phage distal end and the major coat protein p8, present much more abundantly all over

Received: January 2, 2013
Accepted: September 30, 2013

   dx.doi.org/10.1021/ac402192k | *Anal. Chem.* XXXX, XXX, XXX−XXX

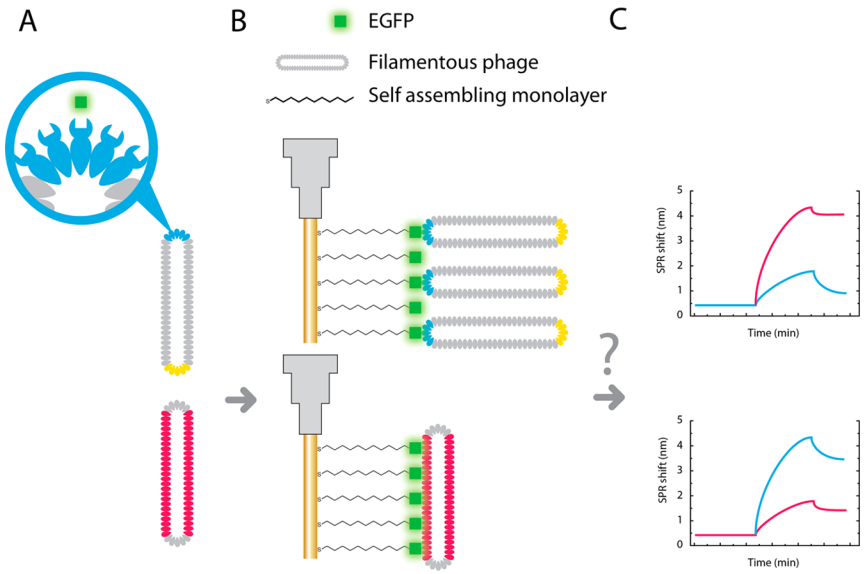

Figure 1. Concept of fiber optic SPR based screening for eGFP-binding phages. (A) Visualization of the filamentous phages, displaying peptides selective for eGFP either at the N-terminus of the p3 protein (blue) or p8 protein (red). Each individual coat protein expresses one peptide. The p9 protein is marked solely for clarification (yellow). (B) Measurement concept with the FO-SPR sensor coated with the eGFP protein (green) and interaction with the two types of phages; the expression of peptides on p3 or p8 proteins can have a strong influence on the affinity of the filamentous phage and consequently their orientation when bound to the FO-SPR sensor surface. (C) The two expected sensorgrams are visualized with red and blue curves, corresponding to the p8 and the p3 peptide, respectively.

the virus surface with up to 2700 copies.[10] Normally these phages display a library of peptides,[11] used to select individual high affinity ligands in a procedure called panning. Here, the phage display library,[11a] consisting of different peptides expressed on the bacteriophage surface as part of their coat proteins, is used to present the peptides to targets of interest with the aim of selecting those peptides with the strongest affinity. Thus, p8 expressing phages were used in the past only to select peptides with lower affinities, as their dense packing on the surface results in a stronger binding due to avidity masking low individual peptide affinity.[12] However, with the trend of implementing whole phages as receptors on biosensors,[13] p8 expressing phages have become valuable due to the advantages of high receptor valence, rivaling high affinities and binding capacity of p3 expressing phages or classic affinity labels such as antibodies. Furthermore, phages can have few clear advantages in such applications compared to nano- and microparticles with high receptor density. First, they can be directly used as a scaffold for the peptide affinity labels.[5,6,14] Second, phages can be easily produced while the peptides remain confined to their original conformation used during the peptide selection phase, which can be crucial for the peptide function.[15]

Despite numerous advantages of using the entire phage as a receptor rather than the individual peptides, binding kinetics of complete phage particles have never been studied in detail. In this article, we will use an in house developed fiber-optic surface plasmon resonance (FO-SPR) biosensor[16] to study the affinity and binding kinetics of phages. Moreover, we will evaluate if dense packing of the peptides on phage surfaces truly results in increased affinity by means of avidity as has been theorized multiple times.[17] As illustrated in Figure 1, we will study whether the location of the expressed peptides on the phage p3 or p8 coat protein is influencing the affinity toward a target molecule or whether it is primarily influencing the orientation on the FO-SPR sensor surface. This will be discerned by analyzing different phases of SPR measurements during phage binding. It can be expected that expression of affinity peptides on the p8 coat proteins will result in a phage orientation closer to the biosensor surface and an increase of the sensor signal, which will mainly disturb the initial phase of the SPR measurement, used to determine the association rate (k_{on}). On the other hand, monitoring of the dissociation rate (k_{off}), will give a better insight in the actual influence of high valence on the affinity of the phages, as high valence results in very low dissociation.[18]

As a model system, we used phages panned with affinity for enhanced Green Fluorescent Protein (eGFP). This 256 amino acid eGFP is a common protein label for both *in vivo* and *in vitro* experiments.[19] Because of the widespread use of eGFP, phages with affinity for this protein can be used for different applications, such as purification and extraction of recombinant eGFP labeled proteins, much in the same way as protein A or G are used as a universal affinity label for antibodies.[20] To the best of our knowledge, this is the first attempt to develop a peptide affinity label with a high binding affinity for eGFP.

MATERIALS AND METHODS

Phage Panning. Depending on the phage library used (Table S1 in the Supporting Information), two different panning strategies were followed: (1) For the linear 6-mer (p3L6), 15-mer (p3L15), and cyclic 6-mer (p3C6) phage display libraries, a tube panning procedure was applied as described earlier.[21] Briefly, after coating eGFP (5 μg/mL) in immuno-tubes followed by post coating with 0.4% milk powder in PBS, the phage libraries were incubated overnight at 4 °C (or 2.5 h at room temperature (RT) for the next rounds). Subsequently the tubes were washed to remove unbound phage and eluted with 0.1 M glycine pH 2.0 for 10 min. The eluted phages were neutralized and incubated with *Escherichia coli*-TG1 cells (Stratagene, Diegem, Belgium) cells at 37 °C for 30 min. Infected cells were plated on agar-tetracycline plates for

dx.doi.org/10.1021/ac402192k | *Anal. Chem.* XXXX, XXX, XXX−XXX

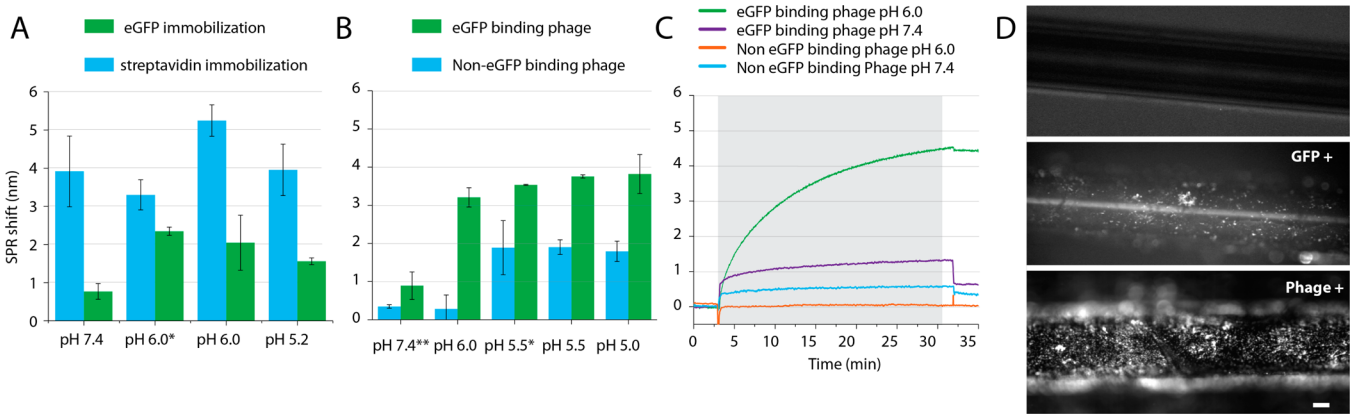

Figure 2. Influence of pH and ionic strength on the binding of phages to eGFP using FO-SPR: (A) optimization of streptavidin and eGFP binding at different pH values and in the presence of 300 mM (∗) NaCl (n = 4); (B) binding of an eGFP-specific or control phage clone at different pH values and in the presence of 137 (∗∗) or 300 mM (∗) NaCl (n = 4). Error bars indicated are the standard deviations of the mean; (C) SPR-binding curves of an eGFP-specific and control phage clone at pH 6.0 and 7.4; (D) microscopy images of the FO-SPR sensor probe with biotin SAM FO-SPR probe (top), after eGFP immobilization (middle), and after phage binding (bottom). Scale bar = 100 μm.

phage amplification. (2) The linear 9-mer landscape (p8L9-LS) library was panned as described earlier.[22] The method was identical to the above-described method for p3 phages except for the usage of a microtiter plate instead of immuno-tubes. Furthermore the eluted phages were neutralized and incubated with "starved" *E. coli* K91 BluKan cells at RT. Infected cells were further grown in NZY-tetracycline-medium (Sigma Aldrich, Bornem, Belgium) in an overnight incubation step at 37 °C.

For both p3 and p8 phages, three rounds of selection were performed. From the third panning round, single clone phages were isolated, identified (through DNA sequencing), and tested for binding to eGFP using ELISA and FO-SPR technology. All selected phages were finally stored in PBS-5% glycerol (w/v%) at −20 °C until further use. The exact peptide sequence of all phages used in this article can be found in Table S2−S5 in the Supporting Information.

SPR Biosensor. The FO-SPR biosensor was optimized and used as described in detail previously.[16,23] A summary can be found in the Supporting Information.

FO-SPR Sensor Probe Preparation. The gold sensing layer of the FO-SPR sensor probe was functionalized with a self-assembling monolayer (SAM) to couple biomolecules on the sensor probe. The SAM consisted of alkane thiol chains with a biotin functional headgroup (Dojindo Molecular Technologies, Munich, Germany). During an overnight incubation (1 μM of thiols in ethanol), the thiol groups attached to the gold surface, while the alkane chains oriented themselves into a well-organized monolayer. After 12 h of incubation, the probes were rinsed in ethanol to remove any unbound alkane thiols and were stored at 4 °C prior to use. For binding biotinylated eGPF on the sensor probe, 10 μg/mL of streptavidin (Invitrogen, Stockholm, Sweden) was immobilized on the SAM biotin groups in 50 mM MES buffer with pH 6.0. The surface was washed with rinsing solution (50 mM NaOH, 1 M NaCl) to remove all nonspecifically bound molecules, followed by binding of biotinylated eGFP (10 μg/mL).

FO-SPR Measurements of Phage Binding. For screening, phages were serially diluted 2-fold starting from 2×10^{12} phages/mL. Both phage binding and phage dissociation to and from the eGFP coated sensor probe, respectively, were monitored for 15 min in 100 μL volumes. Afterward, the FO-SPR sensor probe was regenerated for 60 s in phosphate washing buffer (PBS, 0.1% Tween 20, 1 M NaCl) under continuous stirring. In between two measurements, the FO-SPR sensor probe was equilibrated in measurement buffer (MES, 0.1% Tween 20, pH 6.0) during 5 min. Dilution series of two different phages were simultaneously analyzed using two different measurement channels of the FO-SPR device. Moreover, the repetition dilution series of the same phage were analyzed on different measurement channels to minimize FO-SPR sensor probe artifacts. Binding of both biotinylated eGFP and filamentous phages (colored with the intercalating dye Sybr gold, Life Technologies, Oslo, Norway) on the probe surface was characterized using an inverted fluorescence microscope.

ELISA. The wells of a streptavidin coated ELISA plate (Thermo Scientific, Rockford) were incubated with 100 μL of 5 μg/mL biotin-eGFP in TBS for 1.5 h at room temperature and subsequently washed. Afterward, the eGFP-binding phages were added in a concentration of 1×10^{11} phages/mL in MES buffer (pH 6.0, 50 mM, 0.1% Tween 20) for 1.5 h at RT and extensively washed with MES. Next the wells were incubated with rabbit anti fd bacteriophage antibody (Sigma, Bornem, Belgium) at a concentration of 0.66 μg/mL and a secondary antibody, goat anti rabbit-IgG conjugated with alkaline phosphatase (Jackson ImmunoResearch, West-Grove) at a concentration of 0.24 μg/mL for 1 h each at RT in following buffer: 50 mM Tris, 150 mM NaCl, 0.1% Tween 20, 1 mg/mL BSA, pH 7.5. After extensive washing with MES, the substrate, *p*-nitrophenylphosphatein in 1 M diethanolamine, 1 mM $MgCl^{2+}$ pH 9.8 was added to each well. Finally the absorbance at 405 nm was monitored during 15 min using a plate reader (Fluostar Optima, Ortenberg, Germany).

RESULTS

Optimization of the FO-SPR Assay for Phage−eGFP Interaction. Phage affinity toward the target protein, i.e., eGFP in this study, was evaluated in a direct interaction assay using the FO-SPR biosensor. To establish the assay, immobilization of eGFP onto the FO-SPR sensor probe surface was optimized first. Because the eGFP molecule has a tightly packed barrel structure, which makes functional groups less accessible,[24] immobilization was done through biotin and

dx.doi.org/10.1021/ac402192k | *Anal. Chem.* XXXX, XXX, XXX−XXX

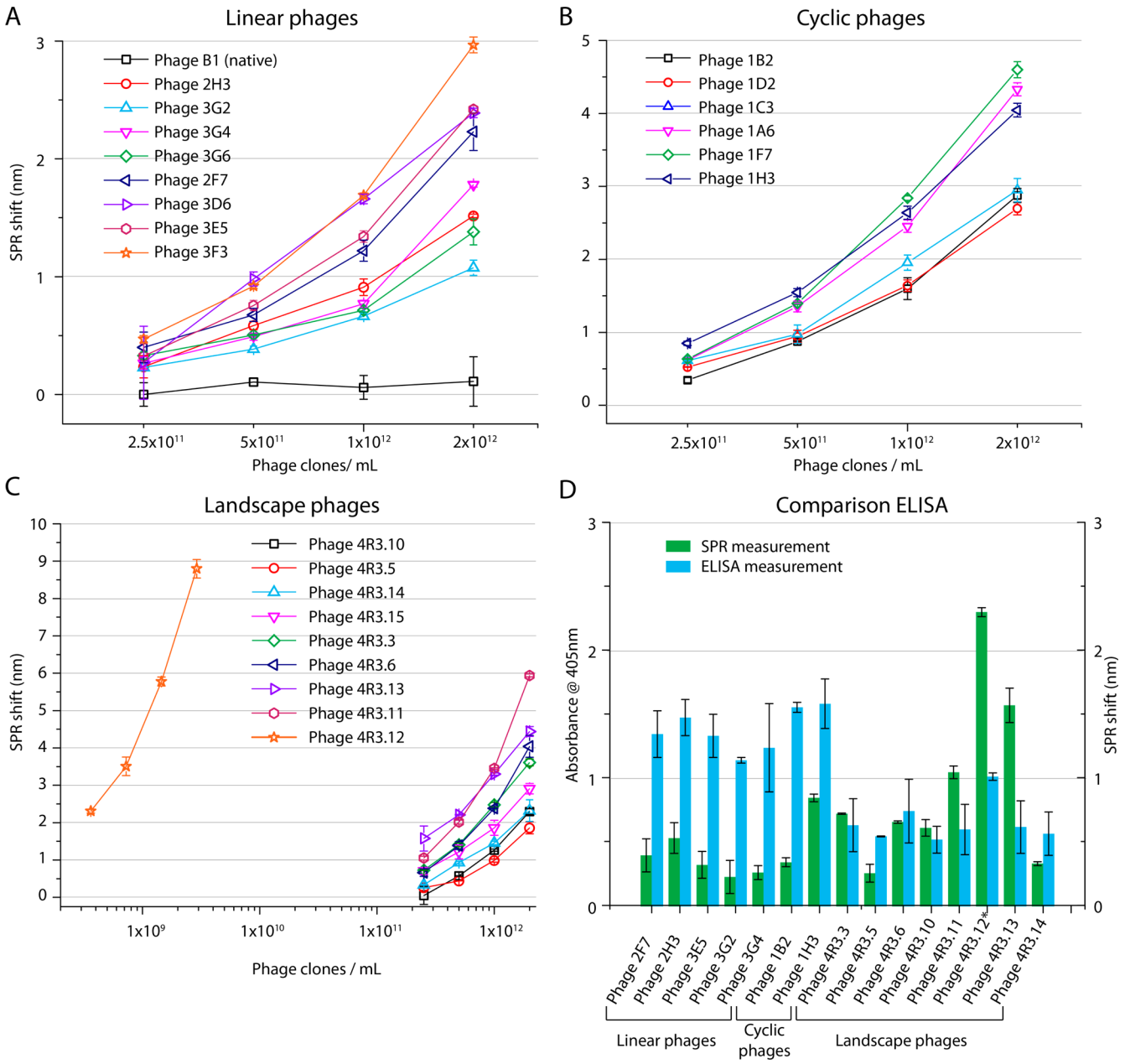

Figure 3. Binding of phage clones to eGFP as determined with FO-SPR: (A) non-eGFP panned native phage together with the linear p3 expression phages; (B) the p3 phages expressing a cyclic peptide; (C) the p8 expressing landscape phages; (D) comparison of phage binding (10^{11} phages/mL) with eGFP as obtained with ELISA and FO-SPR; (∗) phage clone measured at a lower concentration with FO-SPR (10^{8} phages/mL) (n = 4, error bars represent the standard deviation of the mean).

streptavidin. Thus, eGFP was labeled with a small biotin molecule in solution before being bound to a streptavidin molecule on the SPR sensor. This resulted in a higher immobilization efficiency due to use of a modification reaction in free solution rather than directly on the sensor surface, which is known to cause steric hindrance and electrostatic repulsion.[25] Moreover, the tetramer structure of streptavidin[26] holds an extra advantage, as multiple eGFP biotin molecules can be immobilized on one streptavidin molecule.

The streptavidin immobilization was tested in buffered solutions: MES (pH 6), PBS (pH 7.4), acetic acid (pH 5.2) in order to achieve optimal protein density on the probe surface (Figure 2A, blue bars). According to the SPR signal, the highest streptavidin density was realized in MES buffer with pH 6.0. This result is in accordance with the pI for both streptavidin (pI = 6.3)[27] and biotin (pI = 3.5),[28] making both molecules oppositely charged at pH 6.0, allowing them to diffuse closely to the surface which increases the chances for a binding event.[29] Although these molecules should be even more oppositely charged at pH 5.2, a lower binding was observed. This can be explained through charges generated on the FO-SPR sensor surface as a result of deprotonated SAM functional groups at this pH, repelling the highly charged streptavidin molecules. In a similar experiment, differences in the immobilization efficiency of biotinylated eGFP appeared to be much more pronounced (Figure 2A, green bars). For instance, at pH 7.4 a shift of less than 1 nm was observed, whereas lowering the pH to 6.0 doubled the amount of eGFP on the probe surface. By

dx.doi.org/10.1021/ac402192k | Anal. Chem. XXXX, XXX, XXX−XXX

introducing extra ions in this buffer, the density on the FO-SPR surface was further improved and a better reproducibility was achieved (Figure 2A, pH 6.0*).

Subsequently, one of the phage clones panned for eGFP (1B2-p3 phage) was randomly selected for optimizing phage binding to eGFP on the FO-SPR sensor probe surface (Figure 2B). In a standard PBS buffer with pH 7.4, a minor SPR signal shift was visible at a concentration of 5×10^{13} phages/mL, which was only marginally higher than the SPR signal of a non-eGFP selected control phage. In fact, a large part of the FO-SPR signal shift can be attributed to the glycerol matrix of the phage storage buffer, as glycerol has a higher refractive index[30] than the measuring buffer. The low binding signals of phages can be explained by negative charges of eGFP on the probe surface, as well as on the phage surface at pH 7.4, which prevents binding interactions. Knowing that eGFP has a p*I* around pH 6.0,[31] while the filamentous phages have a p*I* around 4.0,[32] buffers with a similar pH were applied (pH 5−7.4) in order to decrease the charges on both surfaces. Results show that by lowering the pH, the SPR signal steadily increased, reaching saturation at pH 5.0 (Figure 2B). However, the affinity of a non-eGFP selected control phage also increased with decreasing pH, but with a different pH-sensitivity compared to the eGFP binding phages. On the basis of these experimental results, a pH of 6.0 is chosen since it results in the highest specific binding. Addition of ions such as Na^+ and Cl^-, another often-used strategy to facilitate molecules to reach their targets,[33] did not affect binding of selected or control phages considerably (Figure 2B). An actual sensorgram for the optimized binding of the selected phage is shown in Figure 2C. The SPR signal of phage binding at pH 6.0 increased approximately 10 times compared to pH 7.4, irrespective of a 10-fold lower phage concentration that is applied at pH 6.0 (1×10^{12} phages/mL) in order to prevent sensor saturation. The optimized conditions were further confirmed with fluorescence microscopy (Figure 2D). Increasing intensity of fluorescence is visible after binding eGFP and fluorescently labeled filamentous phage 1B2 to the sensor surface.

FO-SPR Screening of Selected Phages with Affinity for eGFP. Using the above-described optimized conditions for binding of phages to the FO-SPR sensor probe surface, both p3 and p8 eGFP panned phages were screened for their affinity toward eGFP. Phage measurements were conducted at four different concentrations in a range of 10^{11}−10^{12} phages/mL. The intrinsic nonspecific binding of a native nonpanned filamentous phage to eGFP was first examined. This interaction appeared to be negligible, even at the highest tested concentration (2×10^{12} phages/mL, Figure 3A). Next, the binding of eGFP panned p3 phage clones was measured. These p3 phages can be distinguished according to the type of peptide they express, being either a linear peptide or a cyclic peptide (by the introduction of cysteine groups which can form disulfide bonds[34]). Although all linear p3 phages showed a clear difference in interaction with eGFP compared to the native phage (Figure 3A), substantially higher SPR signal shifts were noted for the p3 cyclic phages (Figure 3B). Phages expressing cyclic peptides are known to have considerably better affinities than phages expressing linear peptides because of a structurally more stable binding conformation, with limited structural entropy in the unbound state, favoring higher binding affinities.[35] Lastly, p8 phages, known as landscape phages (Figure 3C), showed a remarkably higher affinity for eGFP compared to all p3 phages, with one of the p8 clones (phage 4R3.12) having an affinity higher than any of the other landscape clones.

SPR measurements were further validated with an end point ELISA test (Figure 3D), which showed similar trends for individual clones in both assays. Thus, clones 1H3 and 4R3.12 appeared as one of the best binding p3 and p8 phages, respectively, according to both assays. However, a discrepancy was observed in the overall signal intensity for p3 and p8 phages in the two assays. Whereas p3 phages gave a much higher signal in the ELISA assay than p8 phages, SPR binding signals were a mirror image of these results. Here, an explanation can be found with the underlying mechanisms of the two bioassays: FO-SPR measurements monitor phage clones interactions with eGFP label free, while the ELISA measurements are based on a sandwich type of assay. Therefore, in the ELISA, an antibody against the p8 protein (R@fd-IgG) is used to identify phages, after they have bound to eGFP on the microtiter plate surface. As a result, when the p8 coat protein is expressing peptides selective for eGFP, the epitope for the antibody can be modified, resulting in a lower binding efficiency of the antibody.

Higher SPR binding signals obtained with p8 phages are not only indicating higher affinity/avidity for the eGFP immobilized on the SPR sensor but can also be attributed to the orientation of phages on the sensor surface (Figure 1). Nonetheless, as the number and density of affinity peptides displayed on the p8 coat protein is much higher than in p3 phages, p8 phages are capable of binding multiple times to different eGFP molecules on the sensor surface. Earlier reports on multivalent antibodies showed that avidity mainly results in a decrease in dissociation constant.[36] The same effect should be observed when SPR dissociation kinetics of p8 phages are compared to p3 phages. To evaluate this hypothesis, binding curves of the best binding p3 and p8 phages (being clones 1H3, 1F7, 1A6, 4R.11, 4R.12) were studied in more detail.

Binding Kinetics. For each of the five selected phage clones, the kinetic binding parameters such as association rate (k_{on}) and dissociation rate (k_{off}) were derived from the individual SPR measurements (Figure 4). The ratio of both constants further determined the dissociation constant (K_d) for each phage (summarized in Table 1). K_d values for both p8 phages were at least 1 order of magnitude lower than for the p3 phages, confirming our previous conclusions that p8 phages have a higher affinity for eGFP. Nonetheless, the p3 phages also had a K_d in the picomolar range (Figure 4A−C), which is equivalent to the best performing antibodies.[37] The actual SPR binding curves revealed that the SPR signal is almost a flat line during the dissociation phase of p8 phages, indicating only a minimal amount of dissociation from the sensor surface (Figure 4D,E). This result verified the hypothesis that the increase in affinity of p8 phages is influenced considerably by a change in k_{off}. Surprisingly, p3 phages also displayed a very slow dissociation phase (Figure 4A−C), which indicated that even the five-plex multivalence of the p3 protein has a considerable impact on the affinity, as was also found in earlier work.[38] In a recent publication, highly valent magnetic particles (1 μm diameter), which are comparable to p8 landscape phages, showed very similar binding kinetics and a similar increase in both k_{on} and k_{off} rates as p8 phages. Moreover, the affinity of these magnetic particles toward a protein immobilized on a flat surface (prostate specific antigen) was comparable to the affinity of the p8 phages for eGFP used in this research with K_d-values in the femtomolar range.[8]

dx.doi.org/10.1021/ac402192k | *Anal. Chem.* XXXX, XXX, XXX−XXX

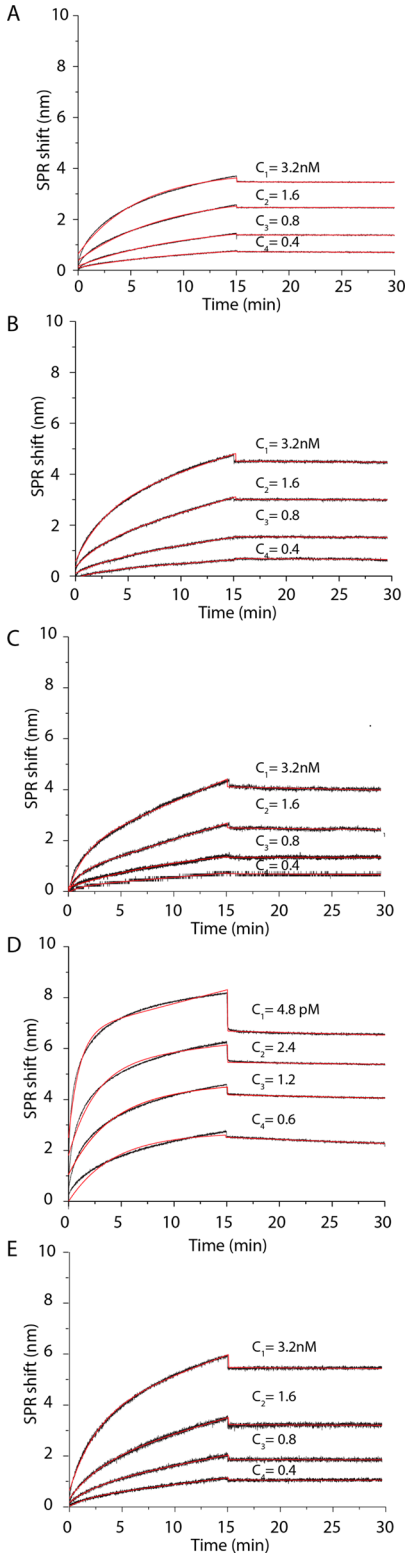

Figure 4. Binding curves of 5 eGFP-binding phage clones with the highest interaction signal in the screening experiment: (A) p3 phage clone 1H3; (B) p3 phage clone 1F7; (C) p3 phage clone 1A6; (D) p8 phage clone 4R3.12; (E) p8 phage clone 4R3.11. The measured signal is depicted in black while fitted curve values for deriving binding parameters are shown in red.

Competitive Assays for Testing the Specificity of the Phage–eGFP Interactions. The specificity of the highest affinity phages (being clones 1F7, 1A6, 4R3.11, and 4R3.12) toward eGFP was evaluated in two different assays.

In the first assay, eGFP immobilized on the sensor surface was competing for phage binding with free eGFP in solution. Increasing concentrations of free eGFP are likely to decrease the number of phages capable of binding to the sensor, if binding is specific (Figure 5A). As expected, the high peptide

Table 1. Kinetic Parameters of eGFP-Binding Phages Measured by FO-SPR

phage	k_{on} (s^{-1} M^{-1})	k_{off} (s^{-1})	K_d (M)
1H3	$1.2 \pm 0.1 \times 10^{8}$	$2.7 \pm 0.1 \times 10^{-3}$	$2.3 \pm 0.3 \times 10^{-11}$
1F7	$3.8 \pm 0.3 \times 10^{8}$	$4.0 \pm 0.6 \times 10^{-3}$	$1.1 \pm 0.2 \times 10^{-11}$
1A6	$3.6 \pm 0.2 \times 10^{8}$	$6.0 \pm 0.2 \times 10^{-3}$	$1.6 \pm 0.4 \times 10^{-11}$
4R3.12	$1.9 \pm 0.1 \times 10^{11}$	$2.2 \pm 0.1 \times 10^{-3}$	$1.2 \pm 0.1 \times 10^{-14}$
4R3.11	$2.3 \pm 1.1 \times 10^{8}$	$1.0 \pm 0.1 \times 10^{-3}$	$4.5 \pm 0.9 \times 10^{-12}$

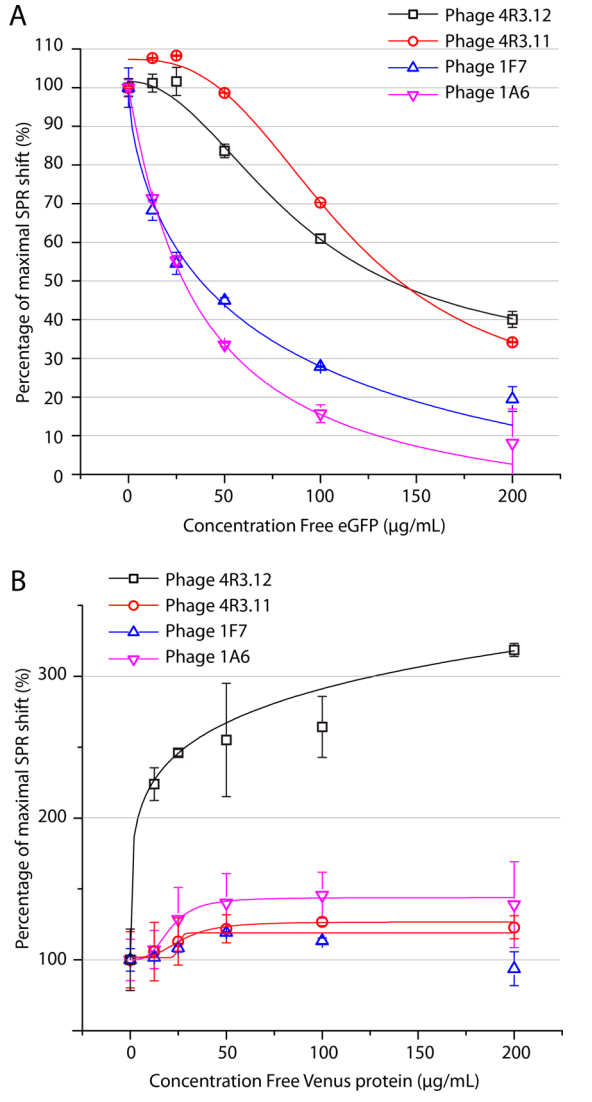

Figure 5. (A) Free eGFP dose-dependently competes with sensor-bound eGFP for binding to phages; (B) highly homologous Venus protein dose-dependently increases the binding signal of eGFP-binding phages bound to the sensor, indicating low affinity interaction of phages with Venus protein. Symbols represent experimental data, while the lines are a logistic sigmoidal fit (n = 4, error bars represent the standard deviation of the mean).

dx.doi.org/10.1021/ac402192k | Anal. Chem. XXXX, XXX, XXX–XXX

densities of the landscape phages made them less prone to inhibition of binding with free eGFP. At moderate concentrations of free eGFP, the capacity of the landscape phages to bind multiple eGFP molecules was further exhibited, when the binding signal even surpassed the maximal signal obtained in the previous experiments. At these concentrations, the landscape phages very likely did bind both free and FO-SPR bound eGFP increasing thus their mass and consequently resulting in a higher SPR-shift. For phage clone 4R3.12, with the highest affinity for eGFP, no complete inhibition of the binding to the FO-SPR sensor was achieved. Even in the presence of 200 μg/mL of free eGFP, this clone was still at 40% of the normal binding signal, indicating that this phage has a high binding capacity. To exclude involvement of any nonspecific sensor surface interaction, an extra test was performed with this phage using a non-eGFP coated sensor surface, which resulted in no binding (Figure S1 in the Supporting Information).

In a second assay, the specificity toward eGFP was tested using an eGFP homologous protein, namely, Venus protein, which differs in only 6 out of 256 amino acids of native GFP (T203Y/F46L/F64L/M153T/V163A/S175G), resulting in a red shift in the emission spectrum of the fluorescent protein.[39] Surprisingly, the Venus protein did not inhibit binding with eGFP on the FO-SPR surface for all 4 phages tested, even at Venus concentrations as high as 200 μg/mL, demonstrating that the phages are indeed highly specific for eGFP. Nevertheless, Venus protein did increase the binding signal indicating a certain degree of cross-reactivity (Figure 5B). For three phages, only a very small shift in SPR binding was recorded above the normal binding signal, suggesting that the phages indeed did bind a small amount of the Venus protein, which increased the density on the sensor surface. In contrast, the signal of clone 4R3.12, increased to 200−300% in the presence of 200 μg/mL Venus protein. This signal increase can only result from high amounts of Venus protein binding to the phage that is already bound to the FO-SPR sensor. However, affinity of this phage for eGFP must be higher than for the Venus protein because the phage is not displaced from the FO-SPR sensor, as was the case for free eGFP in the competitive assay. This corresponds with previous reports showing that affinity molecules developed for "Aequorea victoria"-derived fluorescent proteins, such as eGFP and Venus protein, have affinity for all of these highly homologous proteins.[40]

CONCLUSION

This article presents the first FO-SPR based kinetic analysis of bacteriophage affinities, where phages are used as a whole with either the minor coat protein p3 or the major coat protein p8 expressing peptides selective for eGFP. As expected, the higher peptide densities on the p8 coat protein resulted in a better affinity toward the target protein (eGFP) compared to phages expressing peptides through the p3 coat protein, with K_d values being up to 3 orders of magnitude lower for some p8 phage clones. This difference in affinities could be partially explained with the orientation of p8 phages, as the p8 coat protein expresses affinity peptides throughout the entire phage surface, the phages are positioned with the longer side closer to the sensor surface, which increased the SPR signal during the association phase. Another contributing aspect to such high affinities of p8 phages was the observed decrease in dissociation rate, which is exclusively attributable to multivalent interactions. Nonetheless, p3 phages also express the peptides multivalent, having an especially strong effect on the k_{off} of these phages, resulting in little phage dissociation once bound to eGFP on the sensor surface. SPR measurements, together with the ELISA assays, also revealed considerable differences in eGFP-binding parameters among different p3 and p8 clones, making some phage clones more suited for certain applications than for others. For example, the landscape phage clone 4R3.12 could be well suited for affinity chromatography due to the combination of a good affinity (high k_{on}, low k_{off}) with a high binding capacity. These features would allow easy elution of large amounts of target protein. Furthermore, the fact that this phage clone showed in the competitive assay the highest cross-reactivity for the two "Aequorea victoria"-derived proteins among four tested clones could be used to its advantage. Thus, as a universal recombinant protein affinity label, it can resemble protein A application when used for purification of various antibodies.[41] On the other hand, clone 4R3.11 is much less suited for chromatography as the k_{off} is lower, rendering it less prone for releasing the bound target molecules. Together with its higher specificity, this phage will have better chance for detecting a target, which is more applicable for histology, FACS, or Western blot or even for use in, e.g., phage display mediated immuno-PCR.[42]

ASSOCIATED CONTENT

Supporting Information

Detailed information on the applied materials, methods, and data processing, together with tables containing detailed information on the phage libraries and results on supplementary experiments for binding specificity. This material is available free of charge via the Internet at http://pubs.acs.org.

AUTHOR INFORMATION

Corresponding Author

*E-mail: jeroen.lammertyn@biw.kuleuven.be

Notes

The authors declare no competing financial interest.

ACKNOWLEDGMENTS

This work was funded by the Federal Public Service of Health, Food Chain Safety and Environment (Contract RT 07/06 TUB), KU Leuven Industrial Research Fund (NanoDiag and IOF Mandate N.G. and K.T.), the Flemish Institute for the Promotion of Innovation through Science and Development (IWT Sensors for Food VIS-traject and SB-scholarship K.V.), EFRO financing Interreg NanoSensEU. Design and construction of phage display landscape libraries were supported by Army Research Office ARO/DARPA Grant No. DAAD 19-01-10454 (to V.A.P.) and National Institutes of Health Grants NIH-1 R21 AI05564501 and 1R01 CA125063-01 (to V.A.P.).

REFERENCES

(1) Englund, E. A.; Wang, D.; Fujigaki, H.; Sakai, H.; Micklitsch, C. M.; Ghirlando, R.; Martin-Manso, G.; Pendrak, M. L.; Roberts, D. D.; Durell, S. R.; Appella, D. H. *Nat. Commun.* **2012**, *3*, 614−621.

(2) (a) Grochmal, A.; Ferrero, E.; Milanesi, L.; Tomas, S. *J. Am. Chem. Soc.* **2013**, *135*, 10172−10177. (b) Tomas, S.; Milanesi, L. *Nat. Chem.* **2010**, *2*, 1077−1083.

(3) Perl, A.; Gomez-Casado, A.; Thompson, D.; Dam, H. H.; Jonkheijm, P.; Reinhoudt, D. N.; Huskens, J. *Nat. Chem.* **2011**, *3*, 317−322.

(4) Kecskes, A.; Tosh, D. K.; Wei, Q.; Gao, Z. G.; Jacobson, K. A. *Bioconjugate Chem.* **2011**, *22*, 1115−1127.

(5) Muzard, J.; Platt, M.; Lee, G. U. *Small* **2012**, *8*, 2403−2411.
(6) Nanduri, V.; Sorokulova, I. B.; Samoylov, A. M.; Simonian, A. L.; Petrenko, V. A.; Vodyanoy, V. *Biosens. Bioelectron.* **2007**, *22*, 986−992.
(7) Martinez-Veracoechea, F. J.; Frenkel, D. *Proc. Natl. Acad. Sci. U.S.A.* **2011**, *108*, 10963−10968.
(8) Mani, V.; Wasalathanthri, D. P.; Joshi, A. A.; Kumar, C. V.; Rusling, J. F. *Anal. Chem.* **2012**, *84*, 10485−10491.
(9) Cabilly, S. *Mol. Biotechnol.* **1999**, *12*, 143−148.
(10) Sidhu, S. S. *Biomol. Eng.* **2001**, *18*, 57−63.
(11) (a) Kang, A. S.; Barbas, C. F.; Janda, K. D.; Benkovic, S. J.; Lerner, R. A. *Proc. Natl. Acad. Sci. U.S.A.* **1991**, *88*, 4363−4366. (b) Petrenko, V. A.; Vodyanoy, V. J. *J. Microbiol. Methods* **2003**, *53*, 253−262.
(12) (a) Lowman, H. B. *Annu. Rev. Biophys. Biomol. Struct.* **1997**, *26*, 401−24. (b) de Wildt, R. M.; Tomlinson, I. M.; Ong, J. L.; Holliger, P. *Proc. Natl. Acad. Sci. U.S.A.* **2002**, *99*, 8530−8535. (c) Speck, J.; Arndt, K. M.; Muller, K. M. *Protein Eng. Des. Select.* **2011**, *24*, 473−484. (d) Vrielink, J.; Heins, M. S.; Setroikromo, R.; Szegezdi, E.; Mullally, M. M.; Samali, A.; Quax, W. J. *FEBS J.* **2010**, *277*, 1653−1665.
(13) (a) Penner, G. A. W.; Reginald, M. *Anal. Chem.* **2008**, *80*, 3082−3089. (b) Yang, L. M.; Diaz, J. E.; McIntire, T. M.; Weiss, G. A.; Penner, R. M. *Anal. Chem.* **2008**, *80*, 933−943.
(14) (a) Noppe, W.; Plieva, F. M.; Galaev, I. Y.; Vanhoorelbeke, K.; Mattiasson, B.; Deckmyn, H. *J. Chromatogr., A* **2006**, *1101*, 79−85. (b) Arter, J. A.; Diaz, J. E.; Donavan, K. C.; Yuan, T.; Penner, R. M.; Weiss, G. A. *Anal. Chem.* **2012**, *84*, 2776−2783.
(15) (a) Noppe, W.; Vanhoorelbeke, K.; Galaev, I. Y.; Mattiasson, B.; Deckmyn, H. *J. Dairy Sci.* **2004**, *87*, 3247−3255. (b) Murase, K.; Morrison, K. L.; Tam, P. Y.; Stafford, R. L.; Jurnak, F.; Weiss, G. A. *Chem. Biol.* **2003**, *10*, 161−168.
(16) (a) Pollet, J.; Delport, F.; Janssen, K. P. F.; Jans, K.; Maes, G.; Pfeiffer, H.; Wevers, M.; Lammertyn, J. *Biosens. Bioelectron.* **2009**, *25*, 864−869. (b) Knez, K.; Janssen, K. P. F.; Pollet, J.; Spasic, D.; Lammertyn, J. *Small* **2012**, *8*, 868−872.
(17) (a) Clackson, T.; Hoogenboom, H. R.; Griffiths, A. D.; Winter, G. *Nature* **1991**, *352*, 624−628. (b) Fagerlund, A.; Myrset, A. H.; Kulseth, M. A. *Appl. Microbiol. Biotechnol.* **2008**, *80*, 925−936. (c) Sidhu, S. S.; Fairbrother, W. J.; Deshayes, K. *ChemBioChem* **2003**, *4*, 14−25.
(18) Munoz, E. M.; Correa, J.; Riguera, R.; Fernandez-Megia, E. *J. Am. Chem. Soc.* **2013**, *135*, 5966−5969.
(19) (a) McRae, S. R.; Brown, C. L.; Bushell, G. R. *Protein Expression Purif.* **2005**, *41*, 121−127. (b) Zacharias, D. A.; Violin, J. D.; Newton, A. C.; Tsien, R. Y. *Science* **2002**, *296*, 913−916. (c) Livet, J.; Weissman, T. A.; Kang, H. N.; Draft, R. W.; Lu, J.; Bennis, R. A.; Sanes, J. R.; Lichtman, J. W. *Nature* **2007**, *450*, 56.
(20) (a) Hober, S.; Nord, K.; Linhult, M. *J. Chromatogr., B* **2007**, *848*, 40−47. (b) Akerstrom, B.; Brodin, T.; Reis, K.; Bjorck, L. *J. Immunol.* **1985**, *135*, 2589−2592.
(21) Noppe, W.; Plieva, F.; Galaev, I. Y.; Pottel, H.; Deckmyn, H.; Mattiasson, B. *BMC Biotechnol.* **2009**, *9*, 21.
(22) Brigati, J. R.; Samoylova, T. I.; Jayanna, P. K.; Petrenko, V. A. *Current Protocols in Protein Science*; John Wiley & Sons, Inc.: New York, 2008; Chapter 18, Unit 18.9.
(23) (a) Janssen, K. P.; Knez, K.; Vanysacker, L.; Schrooten, J.; Spasic, D.; Lammertyn, J. *Nanotechnology* **2012**, *23*, 235503. (b) Delport, F.; Pollet, J.; Janssen, K.; Verbruggen, B.; Knez, K.; Spasic, D.; Lammertyn, J. *Nanotechnology* **2012**, *23*, 065503. (c) Pollet, J.; Janssen, K. P.; Knez, K.; Lammertyn, J. *Small* **2011**, *7*, 1003−1006.
(24) Ormo, M.; Cubitt, A. B.; Kallio, K.; Gross, L. A.; Tsien, R. Y.; Remington, S. J. *Science* **1996**, *273*, 1392−1395.
(25) Lu, B.; Smyth, M. R.; OKennedy, R. *Analyst* **1996**, *121*, R29−R32.
(26) Weber, P. C.; Ohlendorf, D. H.; Wendoloski, J. J.; Salemme, F. R. *Science* **1989**, *243*, 85−88.
(27) Burazerovic, S.; Gradinaru, J.; Pierron, J.; Ward, T. R. *Angew. Chem., Int. Ed.* **2007**, *46*, 5510−5514.
(28) Li, X.; Qian, J.; He, S. *Nanotechnology* **2008**, *19*, 355501.
(29) Jans, H.; Jans, K.; Stakenborg, T.; Van de Broek, B.; Lagae, L.; Maes, G.; Borghs, G. *Nanotechnology* **2010**, *21*, 345102.
(30) Beusink, J. B.; Lokate, A. M.; Besselink, G. A.; Pruijn, G. J.; Schasfoort, R. B. *Biosens. Bioelectron.* **2008**, *23*, 839−844.
(31) Sniegowski, J. A.; Lappe, J. W.; Patel, H. N.; Huffman, H. A.; Wachter, R. M. *J. Biol. Chem.* **2005**, *280*, 26248−26255.
(32) Marvin, D. A.; Welsh, L. C.; Symmons, M. F.; Scott, W. R.; Straus, S. K. *J. Mol. Biol.* **2006**, *355*, 294−309.
(33) Pasche, S.; Voros, J.; Griesser, H. J.; Spencer, N. D.; Textor, M. *J. Phys. Chem. B* **2005**, *109*, 17545−17552.
(34) Heinis, C.; Rutherford, T.; Freund, S.; Winter, G. *Nat. Chem. Biol.* **2009**, *5*, 502−507.
(35) Giebel, L. B.; Cass, R. T.; Milligan, D. L.; Young, D. C.; Arze, R.; Johnson, C. R. *Biochemistry* **1995**, *34*, 15430−15435.
(36) (a) Iqbal, U.; Trojahn, U.; Albaghdadi, H.; Zhang, J.; O'Connor-McCourt, M.; Stanimirovic, D.; Tomanek, B.; Sutherland, G.; Abulrob, A. *Br. J. Pharmacol.* **2010**, *160*, 1016−1028. (b) Myung, J. H.; Gajjar, K. A.; Saric, J.; Eddington, D. T.; Hong, S. *Angew. Chem., Int. Ed.* **2011**, *50*, 11769−11772.
(37) Hoogenboom, H. R. *Trends Biotechnol.* **1997**, *15*, 62−70.
(38) (a) Goldman, E. R.; Pazirandeh, M. P.; Charles, P. T.; Balighian, E. D.; Anderson, G. P. *Anal. Chim. Acta* **2002**, *457*, 13−19. (b) Gray, B. P.; Li, S.; Brown, K. C. *Bioconjugate Chem.* **2013**, *24*, 85−96.
(39) Nagai, T.; Ibata, K.; Park, E. S.; Kubota, M.; Mikoshiba, K.; Miyawaki, A. *Nat. Biotechnol.* **2002**, *20*, 87−90.
(40) Shui, B.; Ozer, A.; Zipfel, W.; Sahu, N.; Singh, A.; Lis, J. T.; Shi, H.; Kotlikoff, M. I. *Nucleic Acids Res.* **2012**, *40*, e39.
(41) Hober, S.; Nord, K.; Linhult, M. *J. Chromatogr., B: Anal. Technol. Biomed. Life Sci.* **2007**, *848*, 40−47.
(42) Guo, Y. C.; Zhou, Y. F.; Zhang, X. E.; Zhang, Z. P.; Qiao, Y. M.; Bi, L. J.; Wen, J. K.; Liang, M. F.; Zhang, J. B. *Nucleic Acids Res.* **2006**, *34*, e62.